



Article

Nafion/Surface Modified Ceria Hybrid Membranes for Fuel Cell Application

Polina A. Yurova ¹, Viktoria R. Malakhova ^{1,2}, Ekaterina V. Gerasimova ³ , Irina A. Stenina ¹
and Andrey B. Yaroslavtsev ^{1,*} 

- ¹ Kurnakov Institute of General and Inorganic Chemistry of the Russian Academy of Sciences, Leninsky Prospect 31, 119991 Moscow, Russia; polina31415@mail.ru (P.A.Y.); vika.malakhova.0207@gmail.com (V.R.M.); stenina@igic.ras.ru (I.A.S.)
- ² Basic Department of Inorganic Chemistry and Materials Science, National Research University Higher School of Economics, ul. Myasnitskaya 20, 101000 Moscow, Russia
- ³ Institute of Problems of Chemical Physics of the Russian Academy of Sciences, prospect Academician Semenov 1, 142432 Chernogolovka, Moscow region, Russia; krizhi@gmail.com
- * Correspondence: yaroslav@igic.ras.ru; Tel.: +7-495-952-2487

Abstract: Low chemical durability of proton exchange membranes is one of the main factors limiting their lifetime in fuel cells. Ceria nanoparticles are the most common free radical scavengers. In this work, hybrid membranes based on Nafion-117 membrane and sulfonic or phosphoric acid functionalized ceria synthesized from various precursors were prepared by the in situ method for the first time. Ceria introduction led to a slight decrease in conductivity of hybrid membranes in contact with water. At the same time, conductivity of membranes containing sulfonic acid modified ceria exceeded that of the pristine Nafion-117 membrane at 30% relative humidity (RH). Hydrogen permeability decreased for composite membranes with ceria synthesized from cerium (III) nitrate, which correlates with their water uptake. In hydrogen-air fuel cells, membrane electrode assembly fabricated with the hybrid membrane containing ceria synthesized from cerium (IV) sulfate exhibited a peak power density of 433 mW/cm² at a current density of 1080 mA/cm², while operating at 60 °C and 70% RH. It was 1.5 times higher than for the pristine Nafion-117 membrane (287 mW/cm² at a current density of 714 mA/cm²).

Keywords: Nafion; hybrid membranes; surface modification; ceria; ionic conductivity; fuel cell



Citation: Yurova, P.A.; Malakhova, V.R.; Gerasimova, E.V.; Stenina, I.A.; Yaroslavtsev, A.B. Nafion/Surface Modified Ceria Hybrid Membranes for Fuel Cell Application. *Polymers* **2021**, *13*, 2513. <https://doi.org/10.3390/polym13152513>

Academic Editors: Ying-Ling Liu and Francesco Lufrano

Received: 10 June 2021

Accepted: 27 July 2021

Published: 30 July 2021

Publisher's Note: MDPI stays neutral with regard to jurisdictional claims in published maps and institutional affiliations.



Copyright: © 2021 by the authors. Licensee MDPI, Basel, Switzerland. This article is an open access article distributed under the terms and conditions of the Creative Commons Attribution (CC BY) license (<https://creativecommons.org/licenses/by/4.0/>).

1. Introduction

In recent years, there has been an increasing interest in the modification of cation-exchange membranes by introducing inorganic oxides into the membrane pores and the channels system. Most of the works in this area are devoted to silica and zirconia [1–6], while far too little attention has been paid to ceria [7–9]

During operation of low-temperature fuel cells (FCs), hydrogen peroxide and other reactive oxygen species (hydroxyl radicals, superoxide radicals) are generated in a number of side electrochemical reactions. These radicals cause proton-exchange membranes to degrade and decrease FC power [10–13]. Cerium ions can interact with reactive oxygen species due to the reversible redox reaction $Ce^{4+} \leftrightarrow Ce^{3+}$ [14–17]. Cerium ions can be introduced into the membrane matrix by ion-exchange [18,19] or by casting of the membrane solution with previously prepared CeO₂ nanoparticles [20–22]. The introduction of ceria can also reduce the rate of membrane degradation [19,22–25]. Velayutham et al. showed that Nafion membranes doped with 1 wt% CeO₂ exhibited a decrease in methanol permeability and an increase in conductivity and power density of a methanol fuel cell based on them [26]. However, in many cases, ceria introduction has the opposite effect (proton transport rate, conductivity of hybrid membrane and/or fuel cell performance decrease, at best, does not change) [19,25,27–30].

This is most likely due to the large radius of cerium cations determining the basic nature of ceria surface. Therefore, CeO₂ nanoparticles should form salt bridges with functional groups of membrane pore walls resulting in their crosslinking. This should lead to the exclusion of a part of functional groups from proton transfer and to a decrease in the membrane water uptake as in the case of hybrid membranes with zirconia [31]. A possible way to mitigate the conductivity decrease can be an increase in the acidity of ceria surface by its functionalization with acid groups [32,33]. In some cases, such a modification allows one to increase the conductivity, water uptake, and the selectivity of the prepared hybrid membranes [32,34,35]. Most of the works are devoted to the modification of membranes by acid functionalized silica, titania, or zirconia [32,35–40]. To the best of our knowledge, there is no information on composite membranes doped by ceria with a surface modified by acid groups. At the same time, ceria functionalized by sulfonic or phosphoric acid groups have demonstrated an increase in conductivity by almost two orders of magnitude [41]. This allows us to consider such materials as promising dopants for proton-exchange membranes.

In the present work, hybrid membranes based on Nafion-117 and ceria synthesized from various precursors and functionalized by sulfonic or phosphoric acid groups were prepared for the first time. The proton conductivity and hydrogen permeability of composite membranes as a function of temperature and relative humidity was investigated. In addition, membrane electrode assemblies (MEAs) containing studied membranes were tested.

2. Materials and Methods

The modification of homogeneous perfluorinated sulfonic acid membranes Nafion-117 (thickness of 190–200 µm, Du Pont de Nemours, Wilmington, DE, USA) with ceria was carried out by the in situ method. The following solutions were used as ceria precursors: 0.01 M Ce(NO₃)₃ (Sigma-Aldrich, St. Louis, MO, USA), 0.3 M (NH₄)₂Ce(NO₃)₆ (Sigma-Aldrich, St. Louis, MO, USA), 0.05 M Ce(SO₄)₂ (Sigma-Aldrich, St. Louis, MO, USA), and 0.05 M (NH₄)₄Ce(SO₄)₄ (Sigma-Aldrich, St. Louis, MO, USA).

Before the modification, Nafion-117 membranes were conditioned by sequential boiling in 3% H₂O₂ solution, 5% HCl solution, and deionized water for 2 h. Then, they were placed in a ceria precursor solution for 1 h, treated with a diluted aqueous ammonia solution and re-conditioned by keeping in 5% HCl solution and deionized water at 25 °C for 1 h. Hybrid membranes prepared using Ce(NO₃)₃ and (NH₄)₂Ce(NO₃)₆ solutions were treated with 0.2 or 1 M sulfuric acid or phosphoric acid for modification of the surface of ceria in membrane pores and channels with sulfonic or phosphoric acid groups, respectively. Since oxides of polyvalent elements prepared by precipitation from aqueous precursor solutions are usually nanocrystalline, their surface contains a significant amount of ions sorbed from solutions [42,43]. It can be assumed that ceria precipitation from cerium sulfate solution will lead to a modification of the surface of obtained oxide by sulfonic acid groups. Thus, no additional composite membrane treatment was performed when Ce(SO₄)₂ and (NH₄)₄Ce(SO₄)₄ solutions were used to synthesize ceria. The designations of the prepared hybrid membranes, the precursors of ceria, and the acid used to modify its surface are listed in Table 1.

The cross-sectional morphology of the modified Nafion-117 membranes was studied using a Carl Zeiss NVision 40 scanning electron microscope (SEM) (Carl Zeiss Group, Oberkochen, Germany) equipped with an Oxford X-Max energy dispersive X-ray spectrometry detector (Oxford Instruments, Abingdon-on-Thames, UK). IR-spectra were registered in a Nicolet iS5 FTIR spectrometer (Thermo Fisher Scientific, Waltham, MA, USA) employing a diamond Specac Quest ATR add-on (attenuated total reflection mode). X-ray diffraction patterns were recorded using a Rigaku D/MAX 2200 diffractometer (Rigaku, Tokyo, Japan), CuK_α radiation. Water uptake was determined on a Netzsch TG 209 F1 thermal balance (NETZSCH, Selb, Germany) in platinum crucibles in the temperature range 25–200 °C under argon atmosphere. To determine the dopant content, composite membranes were annealed at 800 °C in air for 0.5 h. The ion exchange capacity (IEC) of

membranes was determined by acid-base titration [44]. The IEC values are given per 1 g of the dry membrane. The conductivity was measured using an impedance analyzer Z1500 PRO Elins (10 Hz–1.5 MHz, Elins LLC, Chernogolovka, Russia) by a two-contact method on symmetric cells with graphite electrodes under an ac signal amplitude of 80 mV. The measurements were carried out in deionized water and at 30% relative humidity (RH) in the temperature range of 25–80 °C. The ionic conductivity at each temperature was obtained using a Nyquist plot from complex impedance analysis. Electronic conductivity was measured at direct current. Hydrogen permeability was studied using a Crystallux-4000M gas chromatograph (RPC Meta-chrom, Co. Ltd, Yoshkar-Ola, Russia) according to the procedure described elsewhere [44]. Mechanical analysis was performed at 25 °C and 32% RH using a Tinius Olsen H5KT universal testing machine (Tinius Olsen, Horsham, PA, USA) with a Tinius Olsen 100R extensometer with 5 mm/min strain rate. Before stress-strain measurements, membrane samples (rectangular specimens of 100 mm length and 10 mm width) were pre-equilibrated at 25 °C and 32% RH. Each measurement was repeated 5 times (five identical samples of each membrane were used).

Table 1. Manufactured hybrid membranes.

Sample	Ceria Precursor	Additional Treatment
Nafion-117	-	-
NC3	0.01 M Ce(NO ₃) ₃	-
NC3_0.2P	0.01 M Ce(NO ₃) ₃	0.2 M H ₃ PO ₄
NC3_1P	0.01 M Ce(NO ₃) ₃	1 M H ₃ PO ₄
NC3_0.2S	0.01 M Ce(NO ₃) ₃	0.2 M H ₂ SO ₄
NC3_1S	0.01 M Ce(NO ₃) ₃	1 M H ₂ SO ₄
NC4	0.3 M (NH ₄) ₂ Ce(NO ₃) ₆	-
NC4_0.2P	0.3 M (NH ₄) ₂ Ce(NO ₃) ₆	0.2 M H ₃ PO ₄
NC4_1P	0.3 M (NH ₄) ₂ Ce(NO ₃) ₆	1 M H ₃ PO ₄
NC4_0.2S	0.3 M (NH ₄) ₂ Ce(NO ₃) ₆	0.2 M H ₂ SO ₄
NC4_1S	0.3 M (NH ₄) ₂ Ce(NO ₃) ₆	1 M H ₂ SO ₄
NC4(S)	0.05 M Ce(SO ₄) ₂	-
NC4(NS)	0.05 M (NH ₄) ₄ Ce(SO ₄) ₄	-

The hybrid membranes were aged *ex situ* using the Fenton reagent (20 ppm Fe(II) in 30 wt% in H₂O₂) prepared immediately before use. A membrane sample (40–50 mg) was stored in the Fenton reagent (20 mL) at 75 °C for 10 h. The fluoride ion concentration in the Fenton reagent after membrane ageing was measured using a Mettler Toledo fluoride ion selective electrode. The fluoride ion selective electrode was calibrated using a series of standard solutions. To keep the pH in the range of 5–7 and prevent complexation of fluoride ions by iron, a total ionic strength adjustment buffer was added to the Fenton reagent solution after membrane ageing.

Membrane electrode assembly (MEA) fabricated with Nafion 117 and NC4(S) membranes were studied in the fuel cell with a working area of 1 cm² (Electrochem, Inc., Woburn, MA, USA). Catalyst ink (weight ratio Nafion®/C is of 0.7) was sprayed onto a surface of a Freudenberg H23C8 gas diffusion layer using a Prism BT setup (USI, Haverhill, MA, USA). Loading of the Pt/C catalyst in the MEA per Pt content was 1.0 mg/cm² (49 wt% Pt/carbon black, Inenergy LLC, Moscow, Russia). The MEAs were fabricated by hot pressing at 130 °C and 80 atm for 3 min. The assembled MEA was tested using a Greenlight Innovation G40 test station at 25 and 60 °C and 100 and 70% RH of the supplied gases, respectively. Gas flow rate was 0.1 L/min for hydrogen and 0.4 L/min for air. Chronoamperograms were measured using an Autolab PGSTAT302 N (Metrohm AG, Utrecht, The Netherlands). The currents changing with a rate < 1%/min were assumed to be steady-state. Before measurements, FCs were kept at 400 mV for 3–8 h to achieve the steady-state performance and optimization of three-phase boundaries.

3. Results and Discussion

Dopant content, ion-exchange capacity, and water uptake of the prepared composite membranes are shown in Table 2. The dopant content was slightly higher in hybrid membranes prepared from a precursor containing cerium in the cationic form ($\text{Ce}(\text{NO}_3)_3$ or $\text{Ce}(\text{SO}_4)_2$ salt) than that for samples obtained from precursors containing cerium in the anionic form ($(\text{NH}_4)_2\text{Ce}(\text{NO}_3)_6$ or $(\text{NH}_4)_4\text{Ce}(\text{SO}_4)_4$ salt), despite the fact that the concentration of $\text{Ce}(\text{NO}_3)_3$ solution was 30 times lower than the $(\text{NH}_4)_2\text{Ce}(\text{NO}_3)_6$ concentration. This effect was also clearly seen for membranes prepared from the solutions of cerium sulfate and cerium-ammonium sulfate of the same concentration. This is explained by the fact that cation-exchange membranes adsorb cations to a much greater extent than anions. When ceria precipitated from $\text{Ce}(\text{NO}_3)_3$ was treated with NaH_2PO_4 or NaHSO_4 solution, cerium(III) phosphate or cerium(III) sulfate was formed [41]. Similar processes can occur in the NC3 hybrid membrane treated with dilute phosphoric or sulfuric acid. The dopant content was significantly higher in the NC3_0.2P membrane than in the NC3 membrane due to CePO_4 formation, the molar mass of which is higher than the molar mass of CeO_2 . Similarly, treatment of the NC3 membrane with 0.2 M H_2SO_4 solution led to $\text{Ce}_2(\text{SO}_4)_3$ formation and the dopant content remained almost unchanged. With increasing the concentration of acids (up to 1 M), the dopant (ceria) was partially dissolved, and its content in the composite membranes decreased. Indeed, when freshly precipitated ceria was treated with 1 M H_2SO_4 , its partial dissolution was observed, while a CeO_2 sample, kept in air for a month, was much less prone to dissolution when treated with acids.

Table 2. Dopant content (ω_{dop}), ion-exchange capacity (IEC) and water uptake ($\omega_{\text{H}_2\text{O}}$) at 95 and 30% RH of the prepared hybrid membranes.

Sample	ω_{dop} , %	IEC \pm 0.02, mmol/g	$\omega_{\text{H}_2\text{O}}$, % (RH = 95%)	$\omega_{\text{H}_2\text{O}}$, % (RH = 30%)
Nafion-117	-	0.91	23.2	5.3
NC3	2.2	0.80	23.7	4.7
NC3_0.2P	2.4	0.81	23.8	4.5
NC3_1P	1.8	0.83	23.9	4.5
NC3_0.2S	2.1	0.81	24.0	4.5
NC3_1S	1.3	0.84	24.2	4.5
NC4	0.8	0.85	26.2	4.9
NC4_0.2P	0.6	0.87	26.0	4.9
NC4_1P	0.5	0.88	26.3	5.0
NC4_0.2S	1.0	0.85	26.0	4.5
NC4_1S	0.9	0.87	26.9	4.4
NC4(S)	0.4	0.89	26.4	5.5
NC4(NS)	0.1	0.88	26.6	5.1

According to the X-ray diffraction data, the residues of all composite membranes after annealing at 800 °C are represented by CeO_2 without any impurity of cerium phosphate or cerium sulfate (Figure S1). At the same time, the IR spectra of the membrane residues showed rather intense bands in the region of 1000–1200 cm^{-1} , corresponding to the vibrations of the SO_4^- and PO_4^- groups (Figure 1). This indicates that only the surface of ceria in the membrane pores and channels was modified. It can be assumed that sulfonic acid groups can also be grafted onto the ceria surface during annealing from SO_3^- groups of the Nafion-117 membrane. However, there are no bands in the region of SO_3^- group vibrations in the IR spectrum of the NC3 membrane residue (Figure 1). It should be noted that IR spectra of composite sulfonic acid membranes are not informative when studying the modification with dopants containing sulfonic acid or phosphate groups, since in the region 1000–1100 cm^{-1} , there is an intense band corresponding to the vibrations of SO_3^- groups of the Nafion-117 membrane.

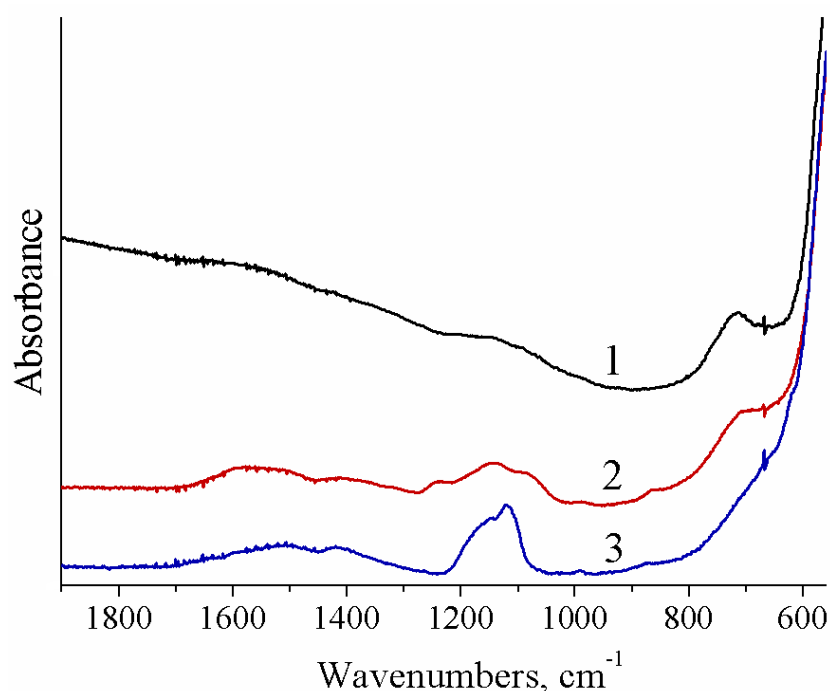


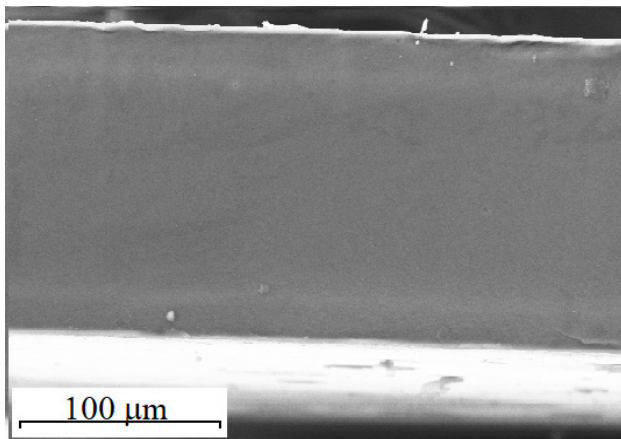
Figure 1. IR spectra of residues of the NC3 (1), NC3_0.2P (2), and NC3_1S (3) hybrid membranes after annealing at 800 °C.

The ion-exchange capacity of all hybrid membranes was lower than that of the pristine Nafion-117 membrane (Table 2). This may be due to the fact that in hybrid membranes, some sulfonic acid groups are bound by strong salt bridges with cerium ions on the surface of CeO_2 nanoparticles and do not take part in other ion-exchange reactions. Similar interactions of acetic acid with ceria surface were described elsewhere [45]. At the same time, the ion-exchange capacity for most composite membranes was almost the same.

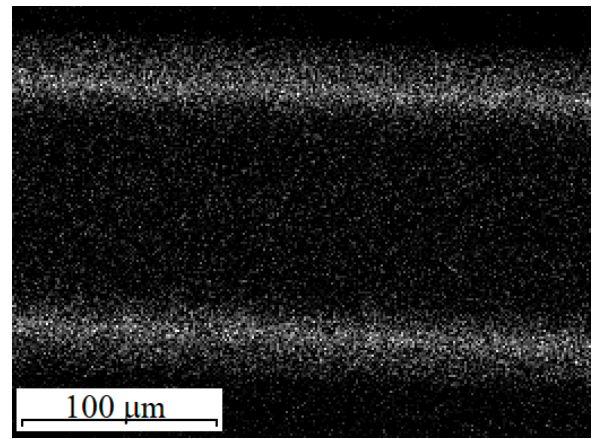
The water uptake of the NC3 membrane did not differ from that of the pristine Nafion-117 membrane (Table 2). The treatment of ceria in membrane pores with phosphoric acid did not lead to noticeable changes in the water uptake of the composite membrane, while the treatment with sulfuric acid resulted in its increase. The water uptake of all hybrid membranes prepared from precursors containing Ce(IV) was slightly higher than the water uptake of the Nafion 117 membrane, and for all hybrid membranes it increased with an increase in the concentration of the acid used for the membrane treatment. The water uptake of all membranes kept at 30% relative humidity (RH) for 7 days decreased more than four times. Moreover, for the composite membranes, this drop was more pronounced than for the pristine Nafion-117 membrane. At the same time, it is surprising that the NC4(S) membrane, which exhibited the best conductivity at 30% RH, had one of the lowest water uptake at this relative humidity.

Figure 2 shows the cross-section SEM images and corresponding EDS cerium mappings of the composite membranes. For all the composite membranes of the NC4 series, the distribution of ceria over the membrane thickness was uniform, while in the composite membranes of the NC3 series, the dopant was concentrated in the near-surface region (Figure 2). The reason is that in the case of the $\text{Ce}(\text{NO}_3)_3$ or $\text{Ce}(\text{SO}_4)_2$ precursor use, cerium cations, as described above, form strong bonds with the sulfonic acid groups of the Nafion-117 membrane, which prevents their further movement into the membrane. On the contrary, the anionic forms of cerium ($\text{Ce}(\text{NO}_3)_6^{2-}$ or $\text{Ce}(\text{SO}_4)_4^{4-}$) are rather easily transferred through the electrically neutral solution located in the pore centers, which leads to the uniform distribution of cerium over the hybrid membrane thickness. However, due to the Donnan exclusion, the anion concentration is low in the cation-exchange membrane, which is confirmed by the low dopant content in the composite membranes prepared using precursors containing cerium in the anionic form (Table 2). On the other hand, cerium

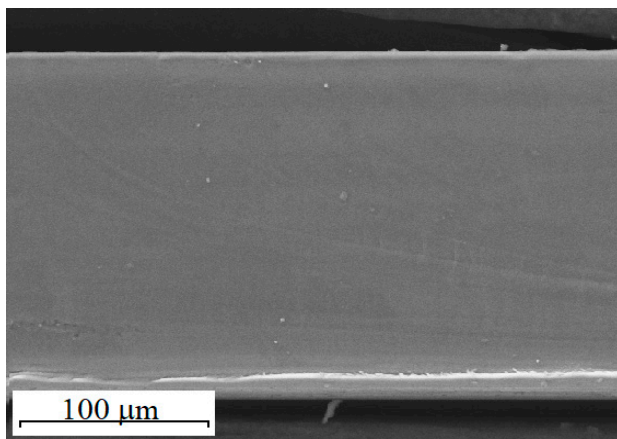
sulfate is stable in aqueous solutions only at low pH values. Its hydrolysis occurs even when the membrane is kept in the $\text{Ce}(\text{SO}_4)_2$ solution (without ammonia treatment), as evidenced by the solution turbidity. Thus, cerium ions can transfer into the membrane as part of hydroxosulfocomplexes with a low charge, which leads to their uniform distribution over the membrane thickness.



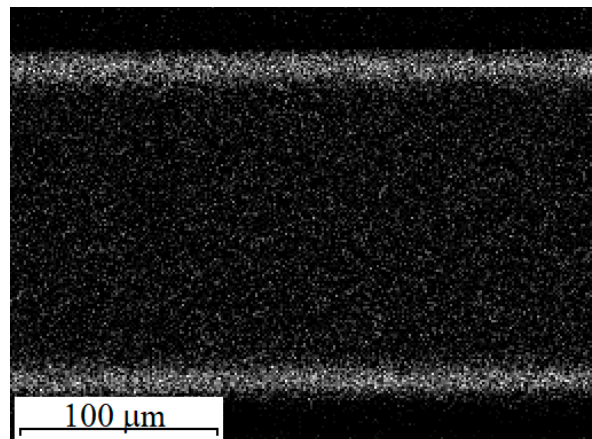
(a)



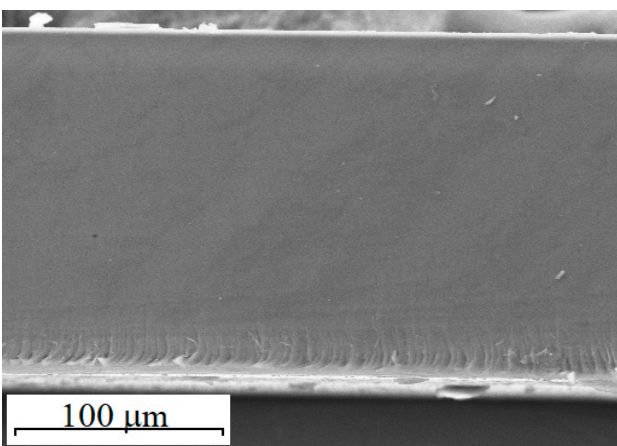
(b)



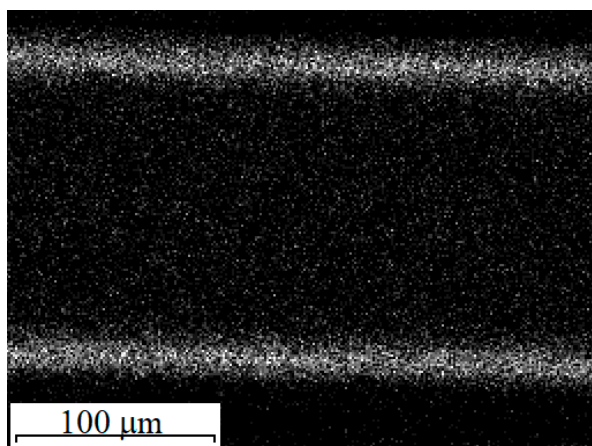
(c)



(d)



(e)



(f)

Figure 2. Cont.

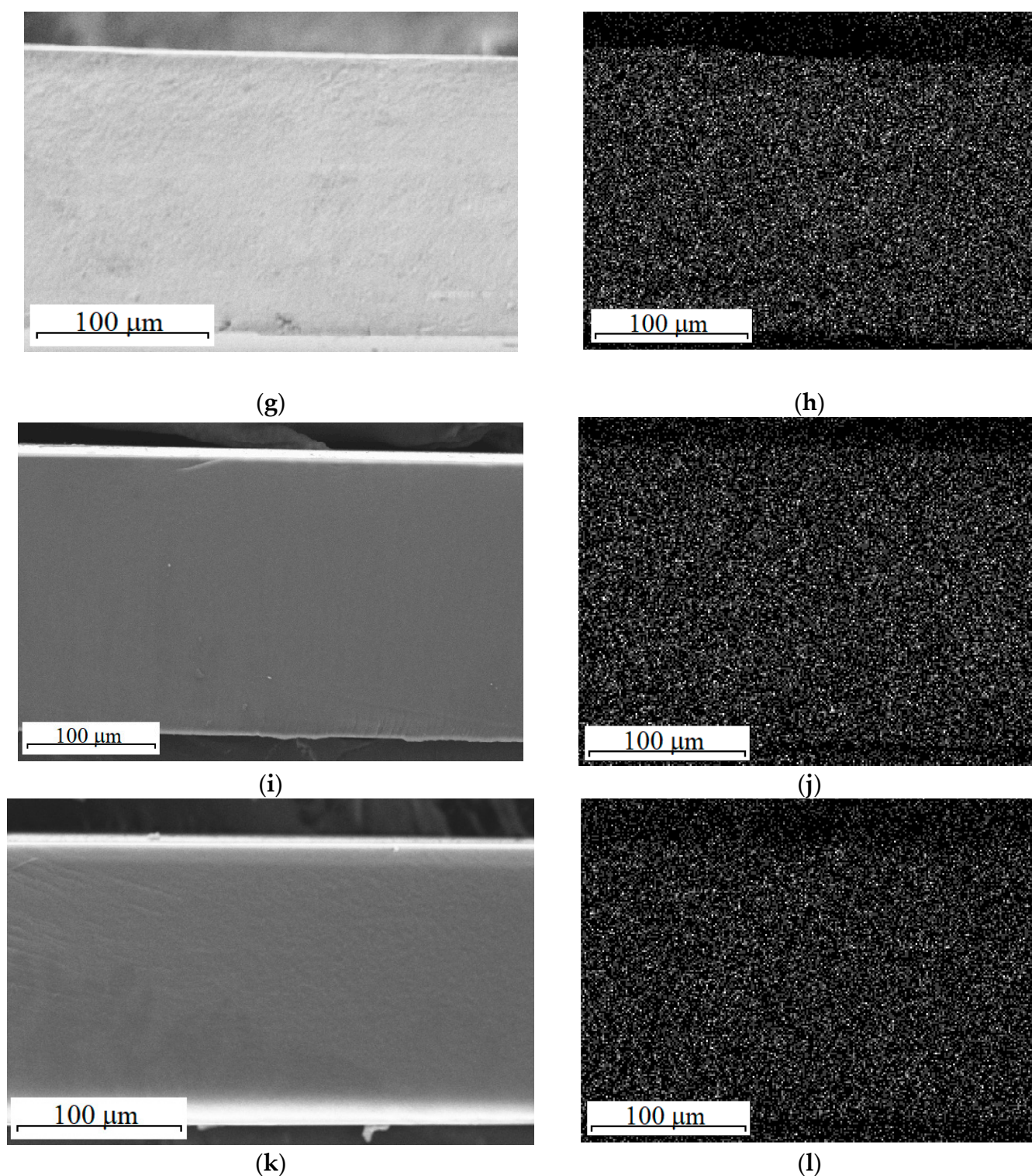


Figure 2. The cross-section SEM images (a,c,e,g,i,k) and EDS cerium mappings (b,d,f,h,j,l) of the NC3 (a,b), NC3_1HP (c,d), NC3_1HS (e,f), NC4 (g,h), NC4(S) (i,j), and NC4(NS) (k,l) composite membranes.

SEM resolution is not sufficient to see particles incorporated into the pores of homogeneous Nafion membranes by the in situ method. Both the pristine and hybrid membranes looked like homogeneous polymer films on SEM images (Figure 2). Nanoparticles were visible on TEM images, and one of them for the NC3_0.2S hybrid membrane is given in Figure 3.

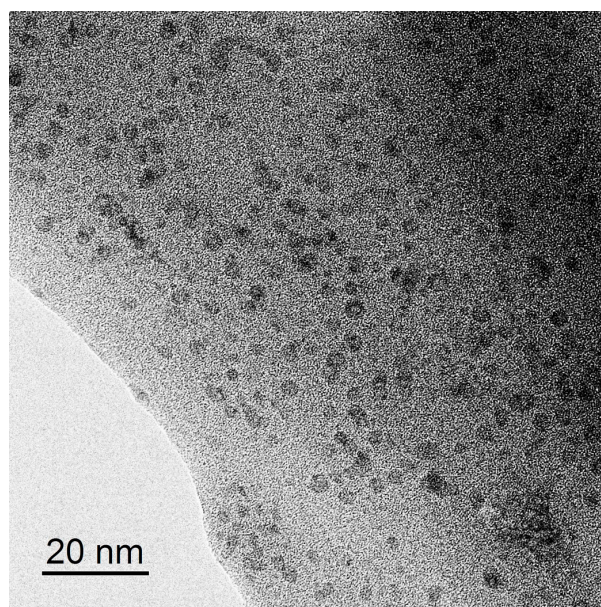


Figure 3. TEM image of the NC3-0.2S hybrid membrane.

The Nyquist plots for the of the NC4(S) composite membrane are shown in Figure S2. The intercept of the Nyquist curves in the high-frequency region with the real resistance axis (Z') represents the through-plane proton transport resistance of the membrane. Such impedance spectra are typical for all membranes under study.

The conductivity of all the hybrid membranes in contact with water was lower than for the pristine Nafion-117 membrane (Figure 4(a1–a3)). The main reason for this is a decrease in the carrier concentration. Despite the higher water uptake, the conductivity of the NC4 series composite membranes was lower than that of the NC3 series samples. Most likely, this is due to the fact that cerium in the NC3 series samples blocks proton transfer only in the surface layer of membrane. For the membranes of both series, the conductivity of the hybrid membranes with ceria modified with phosphate groups was, in general, lower than the conductivity of the composite membranes with CeO_2 modified with sulfonic acid groups, despite the fact that ceria modified by PO_4 -groups ex situ showed higher conductivity [41]. This may be due to the higher water uptake of the composite membranes with ceria modified by SO_4 -groups. In addition, phosphoric acid is significantly weaker than sulfuric acid. Thus, its dissociation in a membrane with high acidity is suppressed. Moreover, phosphate anions on the oxide surface can act as a "trap for protons", limiting their transport. The reason for the relatively low conductivity of NC4(NS) is apparently the partial substitution of protons for ammonium ions of the precursor.

The conductivity of all the hybrid membranes at 30% RH was almost an order of magnitude lower than the conductivity of these membranes in contact with water (Figure 4(b1–b3)), which is due to the partial membrane dehydration (Table 2). However, for the composite membranes with surface-modified ceria, this decrease was less pronounced. Moreover, the NC4(S), NC4(NS), and NC4_1P membranes exhibited higher conductivity compared with the pristine Nafion-117 membrane. It should be noted that this situation is typical for hybrid membranes [34]. The conductivity of all the hybrid membranes at 30% RH was almost an order of magnitude lower than the conductivity of these membranes in contact with water (Figure 4(b1–b3)), which is due to the partial membrane dehydration (Table 2). However, for the composite membranes with surface-modified ceria, this decrease was less pronounced. Moreover, the NC4(S), NC4(NS), and NC4_1P membranes exhibited higher conductivity compared with the pristine Nafion-117 membrane. It should be noted that this situation is typical for hybrid membranes [34].

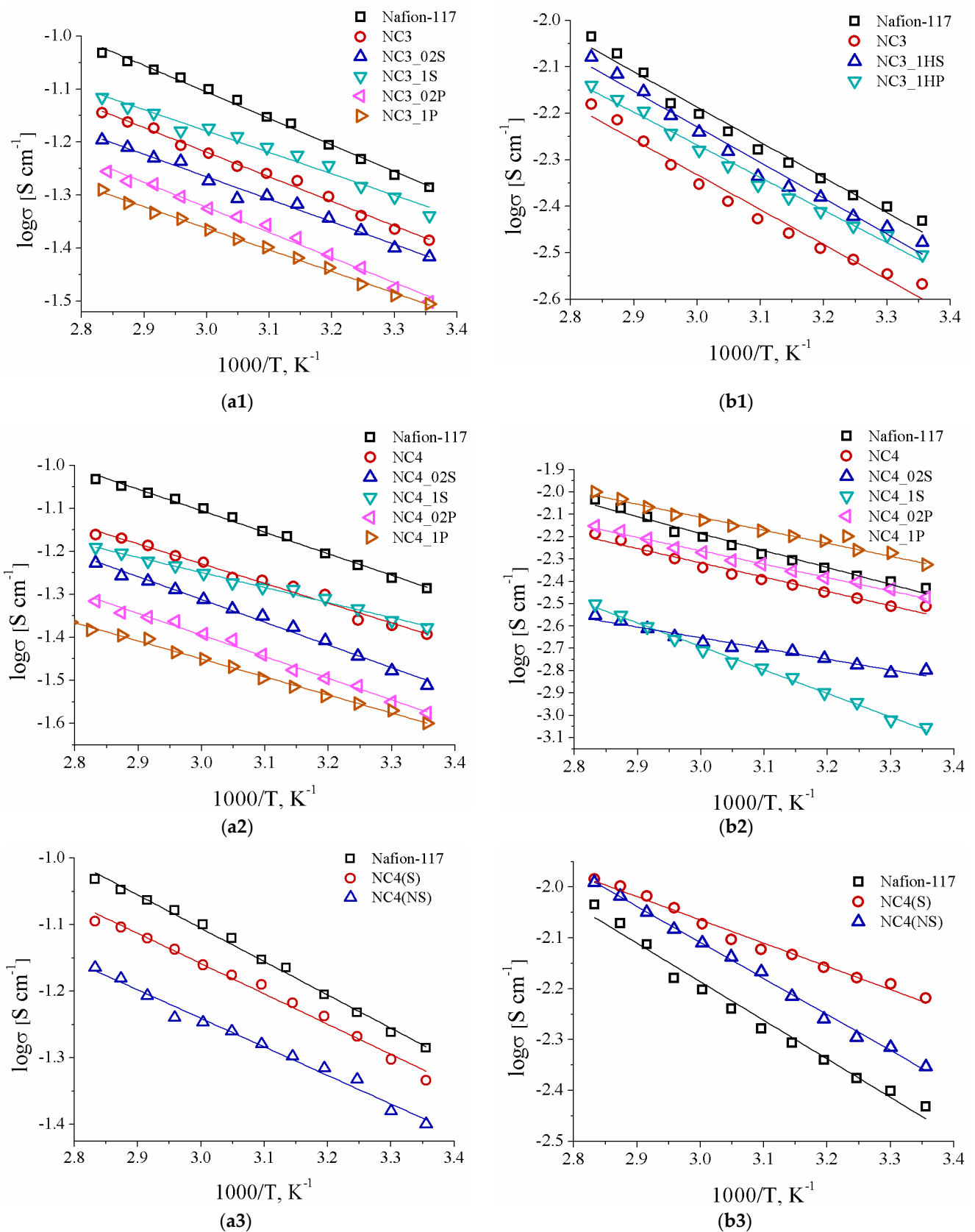


Figure 4. Temperature dependences of conductivity for the prepared hybrid membranes of the NC3 series (a1,b1), the NC4 series (a2,b2), the NC4(S) and NC4(NS) membranes (a3,b3) in contact with water (a1–a3) and at 30% relative humidity (b1–b3).

The hydrogen permeability of the composite membranes at 30 and 100% RH are shown in Figure 5. At 100% RH, the hydrogen permeability for most hybrid membranes turned was higher than in Nafion-117, with the exception of some samples of the Ce3 series. In this case, a significant ceria content in the near-surface membrane layers, as well as a lower water uptake of these membranes, prevented the hydrogen diffusion through the pore solution. With decreasing relative humidity, on the contrary, the hydrogen permeability for many hybrid membranes was lower. The reason for this is that at low RH, the membrane water uptake decreases and the contribution of the Debye layer, from which non-polar gas molecules are displaced, becomes increasingly significant.

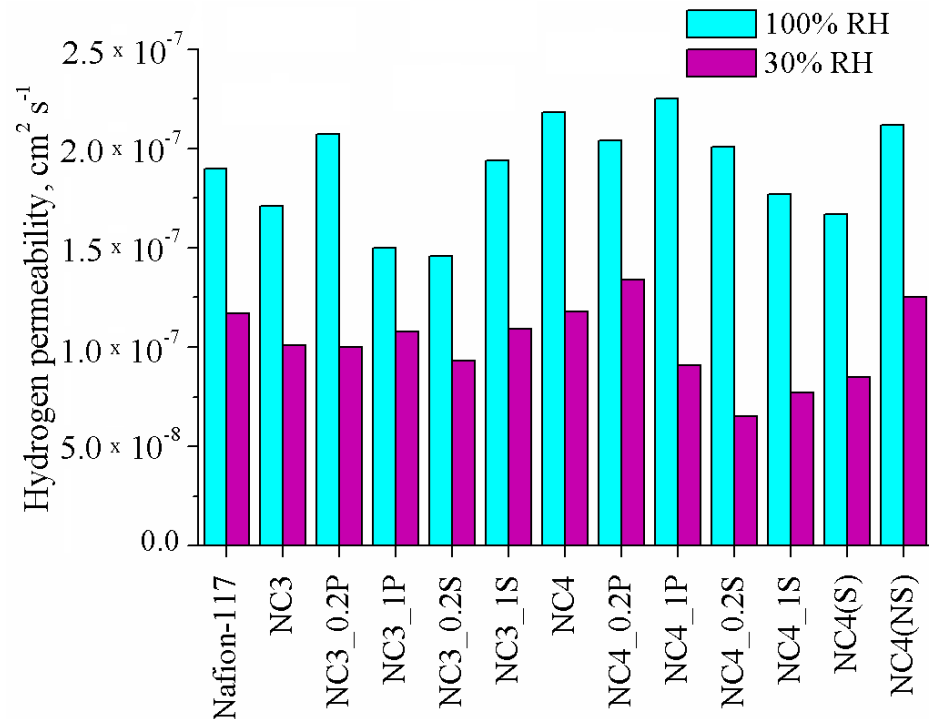


Figure 5. Hydrogen permeability at 30 and 100% RH of the studied composite membranes.

Upon ceria incorporation, the mechanical properties of the hybrid membranes changed slightly (Figure S3). The Young modulus of the pristine Nafion-117 membrane was determined to be 257 ± 4 MPa. It increases slightly up to 260–275 MPa for the hybrid membranes with CeO₂. Ceria incorporation seemed to increase the tensile strength slightly from 33.5 ± 0.4 MPa to 34–37 MPa (for the hybrid membranes). At the same time, the maximum strain for most membranes decreased slightly as compared with the pristine Nafion-117 ($309 \pm 3\%$). However, its magnitude did not decrease below 270%, and even increased to 312% for the NC4(NS) composite membrane. It can be assumed that a slight increase in Young's modulus and tensile strength is determined by insignificant cross-linking of membranes upon dopant introduction, whereas its maximum strain also naturally decreases. We observed similar changes in the mechanical properties upon poly(3,4-ethylenedioxythiophene) introduction into the Nafion membranes [46]. It can be assumed that these changes, at least, will not lead to a deterioration in the mechanical stability of membranes in MEAs.

As it is known, during the operation of low-temperature fuel cells, significant problems arise with membrane hydration, especially in the anode side, from which water molecules are partially transferred away along with protons. Therefore, it was of interest to test such membranes in fuel cells at a slightly reduced humidification. Current-voltage curves and dependences of power density on current density for MEAs with the Nafion-117 and NC4(S) membranes at 25 and 60 °C are shown in Figure 6. In the middle current range, the slope of the current-voltage curves of the MEAs based on the NC4(S) membrane was

reduced compared with the MEAs with the Nafion-117 membrane, which indicates a decrease in the MEA internal resistance. Additionally, and which is not less important, the peak power density also significantly increased for MEAs with the modified membrane. Its values were 233 and 276 mW/cm^2 at 25 °C and 287 and 433 mW/cm^2 at 60 °C for the MEAs with Nafion-117 and the NC4(S) membrane, respectively. An increase in the current density at a voltage of 0.4 V corresponding to the dominance of the influence of ohmic and transport restrictions should also be noted. The MEAs based on Nafion-117 and the modified membrane delivered 582 and 689 mA/cm^2 at 25 °C and 714 and 1080 mA/cm^2 at 60 °C, respectively.

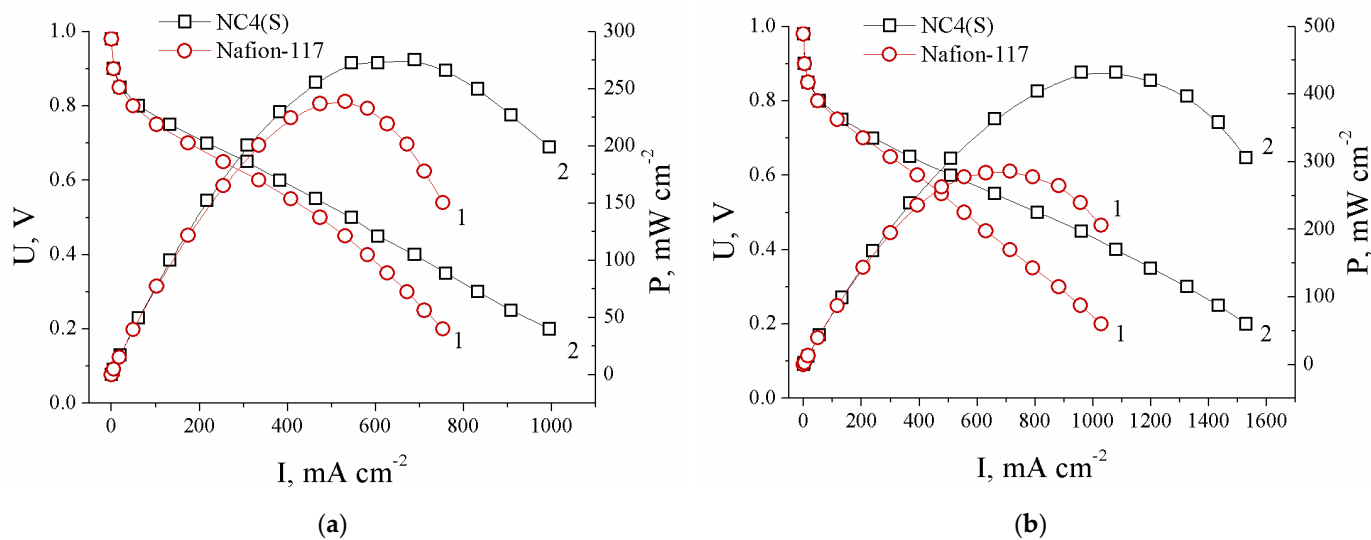


Figure 6. Polarization and power density curves for the MEAs with Nafion-117 (1) and the NC4(S) composite membrane (2) at 25 °C, 100% RH (a), and 60 °C, 70% RH (b).

To test the ability of dopant to mitigate the membrane degradation, the pristine Nafion-117 and the NC4(S) composite membranes were treated with the Fenton solution (ex situ accelerated degradation test). The fluoride emission rate (the ratio between the mass of released fluoride ions and the initial membrane mass) was about four times lower for the NC4(S) membrane than for Nafion-117 (0.42 and 1.81 mg/g , respectively).

4. Conclusions

New composite membranes based on Nafion-117 and ceria with a surface modified by sulfonic acid or phosphate groups were prepared by the in situ method. When cerium (III) nitrate was used as a precursor, the dopant was concentrated in the near-surface layers of the composite membrane, while in the case of $(\text{NH}_4)_2\text{Ce}(\text{NO}_3)_6$, the dopant distribution over the membrane thickness was uniform. At low humidity, the proton conductivity of membranes with ceria modified with sulfonic acid groups exceeded that of the pristine Nafion-117 membrane. Hydrogen permeability decreased for almost all composite membranes with ceria obtained from cerium (III) nitrate, which correlates with their water uptake. Compared to the pristine Nafion-117 membrane, the peak power density of MEAs with the composite membrane containing ceria modified with sulfonic acid groups increased 1.5 times. Taking into account this and high stability of the hybrid membranes in the presence of peroxide moieties, it can be assumed that the prepared hybrid membranes have high potential for hydrogen-air fuel cell applications.

Supplementary Materials: The following are available online at <https://www.mdpi.com/article/10.3390/polym13152513/s1>, Figure S1: X-ray diffraction patterns of residues of the NC3 (1), NC3_1S (2), NC3_1P (3), NC4 (4), NC4_1S (5), and NC4_1P (6) hybrid membranes after annealing at 800 °C, Figure S2: Nyquist plots of the NC4(S) composite membrane recorded at different temperatures in contact with water (a) and 30% RH (b), Figure S3: Stress–strain responses of the pristine Nafion-117 (1) and the NC3 (2), NC4_1P (3), NC4(S) (4), and NC4(NS) (5) hybrid membranes.

Author Contributions: Conceptualization, I.A.S. and A.B.Y.; methodology, P.A.Y. and I.A.S.; investigation, P.A.Y., V.R.M., E.V.G. and I.A.S.; data curation, P.A.Y., I.A.S. and A.B.Y.; writing—original draft preparation, P.A.Y. and I.A.S.; writing—review and editing, I.A.S. and A.B.Y.; supervision, I.A.S. and A.B.Y.; project administration, I.A.S.; funding acquisition, P.A.Y., I.A.S. All authors have read and agreed to the published version of the manuscript.

Funding: This research was funded by the Russian Foundation for Basic Research grant number 19-38-90027.

Institutional Review Board Statement: Not applicable.

Informed Consent Statement: Not applicable.

Data Availability Statement: The data presented in this study are available on request from the corresponding author.

Acknowledgments: Scanning electron microscopy was performed using shared experimental facilities supported by IGIC RAS state assignment.

Conflicts of Interest: The authors declare no conflict of interest.

References

1. Shaari, N.; Kamarudin, S.K. Recent advances in additive-enhanced polymer electrolyte membrane properties in fuel cell applications: An overview. *Int. J. Energy Res.* **2019**, *43*, 2756–2794. [[CrossRef](#)]
2. Ercelik, M.; Ozden, A.; Devrim, Y.; Colpan, C.O. Investigation of Nafion based composite membranes on the performance of DMFCs. *Int. J. Hydrogen Energy* **2017**, *42*, 2658–2668. [[CrossRef](#)]
3. Stenina, I.A.; Yaroslavtsev, A.B. Ionic mobility in ion-exchange membranes. *Membranes* **2021**, *11*, 198. [[CrossRef](#)] [[PubMed](#)]
4. Gashoul, F.; Parnian, M.J.; Rowshanzamir, S. A new study on improving the physicochemical and electrochemical properties of SPEEK nanocomposite membranes for medium temperature proton exchange membrane fuel cells using different loading of zirconium oxide nanoparticles. *Int. J. Hydrogen Energy* **2017**, *42*, 590–602. [[CrossRef](#)]
5. Li, J.; Xu, G.; Luo, X.; Xiong, J.; Liu, Z.; Cai, W. Effect of nano-size of functionalized silica on overall performance of swelling-filling modified Nafion membrane for direct methanol fuel cell application. *Appl. Energy* **2018**, *213*, 408–414. [[CrossRef](#)]
6. Saccà, A.; Carbone, A.; Gatto, I.; Pedicini, R.; Passalacqua, E. Synthesized yttria stabilised zirconia as filler in proton exchange membranes (PEMs) with enhanced stability. *Polym. Test.* **2018**, *65*, 322–330. [[CrossRef](#)]
7. Ketpang, K.; Oh, K.; Lim, S.C.; Shanmugam, S. Nafion-porous cerium oxide nanotubes composite membrane for polymer electrolyte fuel cells operated under dry conditions. *J. Power Sources* **2016**, *329*, 441–449. [[CrossRef](#)]
8. Vinothkannan, M.; Ramakrishnan, S.; Kim, A.R.; Lee, H.K.; Yoo, D.J. Ceria stabilized by titanium carbide as a sustainable filler in the Nafion matrix improves the mechanical Integrity, electrochemical durability, and hydrogen impermeability of proton-exchange membrane fuel cells: Effects of the filler content. *ACS Appl. Mater. Interfaces* **2020**, *12*, 5704–5716. [[CrossRef](#)]
9. Shin, D.; Han, M.; Shul, Y.G.; Lee, H.; Bae, B. Analysis of cerium-composite polymer-electrolyte membranes during and after accelerated oxidative-stability test. *J. Power Sources* **2018**, *378*, 468–474. [[CrossRef](#)]
10. Alavijeh, A.S.; Goulet, M.A.; Khorasany, R.M.; Ghataurah, J.; Lim, C.; Lauritzen, M.; Kjeang, E.; Wang, G.G.; Rajapakse, R.K. Decay in mechanical properties of catalyst coated membranes subjected to combined chemical and mechanical membrane degradation. *Fuel Cells* **2015**, *15*, 204–213. [[CrossRef](#)]
11. Zaton, M.; Roziere, J.; Jones, D.J. Current understanding of chemical degradation mechanisms of perfluorosulfonic acid membranes and their mitigation strategies: A review. *Sustain. Energy Fuels* **2017**, *1*, 409–438. [[CrossRef](#)]
12. Schlick, S. (Ed.) *The Chemistry of Membranes Used in Fuel Cells: Degradation and Stabilization*; John Wiley & Sons, Inc.: New York, NY, USA, 2017.
13. Filippov, S.P.; Yaroslavtsev, A.B. Hydrogen energy: Development prospects and materials. *Russ. Chem. Rev.* **2021**, *90*, 627–643. [[CrossRef](#)]
14. Walkey, C.; Das, S.; Seal, S.; Erlichman, J.; Heckman, K.; Ghibelli, L.; Traversa, E.; McGinnis, J.F.; Self, W.T. Catalytic properties and biomedical applications of cerium oxide nanoparticles. *Environ. Sci. Nano* **2015**, *2*, 33–53. [[CrossRef](#)]
15. Rui, Z.; Liu, J. Understanding of free radical scavengers used in highly durable proton exchange membranes. *Progr. Nat. Sci. Mater. Int.* **2020**, *30*, 732–742. [[CrossRef](#)]

16. Tinh, V.D.; Kim, D. Enhancement of oxidative stability of PEM fuel cell by introduction of HO• radical scavenger in Nafion ionomer. *J. Memb. Sci.* **2020**, *613*, 118517. [[CrossRef](#)]
17. Kumar, A.; Hong, J.; Yun, Y.; Bhardwaja, A.; Song, S.J. The role of surface lattice defects of CeO_{2-δ} nanoparticles as a scavenging redox catalyst in polymer electrolyte membrane fuel cells. *J. Mater. Chem. A* **2020**, *8*, 26023–26034. [[CrossRef](#)]
18. Coms, F.D.; Liu, H.; Owejan, J.E. Mitigation of perfluorosulfonic acid membrane chemical degradation using cerium and manganese ions. *ECS Trans.* **2008**, *16*, 1735–1747. [[CrossRef](#)]
19. Zaton, M.; Prélôt, B.; Donzel, N.; Rozière, J.; Jones, D.J. Migration of Ce and Mn ions in PEMFC and its impact on PFSA membrane degradation. *J. Electrochem. Soc.* **2018**, *165*, F3281–F3289. [[CrossRef](#)]
20. Pearman, B.P.; Mohajeri, N.; Brooker, R.P.; Rodgers, M.P.; Slattery, D.K.; Hampton, M.D.; Cullen, D.A.; Seal, S. The degradation mitigation effect of cerium oxide in polymer electrolyte membranes in extended fuel cell durability tests. *J. Power Sources* **2013**, *225*, 75–83. [[CrossRef](#)]
21. Lim, C.; Alavijeh, A.S.; Lauritzen, M.; Kolodziej, J.; Knights, S.; Kjeang, E. Fuel cell durability enhancement with cerium oxide under combined chemical and mechanical membrane degradation. *ECS Electrochem. Lett.* **2015**, *4*, F29–F31. [[CrossRef](#)]
22. Weissbach, T.; Peckham, T.J.; Holdcroft, S. CeO₂, ZrO₂ and YSZ as mitigating additives against degradation of proton exchange membranes by free radicals. *J. Memb. Sci.* **2016**, *498*, 94–104. [[CrossRef](#)]
23. Trogadas, P.; Parrondo, J.; Ramani, V. Degradation mitigation in polymer electrolyte membranes using cerium oxide as a regenerative free-radical scavenger. *Electrochem. Solid State Lett.* **2008**, *11*, B113–B116. [[CrossRef](#)]
24. Prabhakaran, V.; Ramani, V. Structurally-tuned nitrogen-doped cerium oxide exhibits exceptional regenerative free radical scavenging activity in polymer electrolytes. *J. Electrochem. Soc.* **2014**, *161*, F1–F9. [[CrossRef](#)]
25. Zhao, W.; Haolin, T.; Huijie, Z.; Ming, L.; Rui, C.; Pan, X.; Mu, P. Synthesis of Nafion/CeO₂ hybrid for chemically durable proton exchange membrane of fuel cell. *J. Memb. Sci.* **2012**, *421–422*, 201–210.
26. Velayutham, P.; Sahu, A.K.; Parthasarathy, S. A Nafion-ceria composite membrane electrolyte for reduced methanol crossover in direct methanol fuel cells. *Energies* **2017**, *10*, 259. [[CrossRef](#)]
27. Baker, M.; Williams, S.T.; Mukundan, R.; Spornjak, D.; Advani, S.G.; Prasad, A.K.; Borup, R.L. Zr-doped ceria additives for enhanced PEM fuel cell durability and radical scavenger stability. *J. Mater. Chem. A* **2017**, *5*, 15073–15079. [[CrossRef](#)]
28. Akrouf, A.; Delrue, A.; Zaton, M.; Duquet, F.; Spanu, F.; Taillades-Jacquin, M.; Cavaliere, S.; Jones, D.; Rozière, J. Immobilisation and release of radical scavengers on nanoclays for chemical reinforcement of proton exchange membranes. *Membranes* **2020**, *10*, 208. [[CrossRef](#)] [[PubMed](#)]
29. Donnadio, A.; D'Amato, R.; Marmottini, F.; Panzetta, G.; Pica, M.; Battocchio, C.; Capitani, D.; Ziarelli, F.; Casciola, M. On the evolution of proton conductivity of Aquivion membranes loaded with CeO₂ based nanofillers: Effect of temperature and relative humidity. *J. Memb. Sci.* **2019**, *574*, 17–23. [[CrossRef](#)]
30. Parnian, M.J.; Rowshanzamir, S.; Prasad, A.K.; Advani, S.G. Effect of ceria loading on performance and durability of sulfonated poly (ether ether ketone) nanocomposite membranes for proton exchange membrane fuel cell applications. *J. Memb. Sci.* **2018**, *565*, 342–357. [[CrossRef](#)]
31. Golubenko, D.V.; Shaydullin, R.R.; Yaroslavtsev, A.B. Improving the conductivity and permselectivity of ion-exchange membranes by introduction of inorganic oxide nanoparticles: Impact of acid–base properties. *Colloid Polym. Sci.* **2019**, *297*, 741–748. [[CrossRef](#)]
32. Bakangura, E.; Wu, L.; Ge, L.; Yang, Z.; Xu, T. Mixed matrix proton exchange membranes for fuel cells: State of the art and perspectives. *Progr. Polymer Sci.* **2016**, *57*, 103–152. [[CrossRef](#)]
33. Stenina, I.; Golubenko, D.; Nikonenko, V.; Yaroslavtsev, A. Selectivity of transport processes in ion-exchange membranes: Relationship with the structure and methods for its improvement. *Int. J. Mol. Sci.* **2020**, *21*, 5517. [[CrossRef](#)]
34. Apel, P.Y.; Bobreshova, O.V.; Volkov, A.V.; Volkov, V.V.; Nikonenko, V.V.; Stenina, I.A.; Filippov, A.N.; Yampolskii, Y.P.; Yaroslavtsev, A.B. Prospects of membrane science developments. *Membr. Membr. Technol.* **2019**, *1*, 45–63. [[CrossRef](#)]
35. Wong, C.Y.; Wong, W.Y.; Ramy, K.; Khalid, M.; Loh, K.S.; Daud, W.R.; Lim, K.L.; Walvekar, R.; Kadhum, A.A. Additives in proton exchange membranes for low- and high-temperature fuel cell applications: A review. *Int. J. Hydrogen Energy* **2019**, *44*, 6116–6135. [[CrossRef](#)]
36. Safronova, E.Y.; Stenina, I.A.; Yaroslavtsev, A.B. Synthesis and characterization of MF-4SK+SiO₂ hybrid membranes modified with tungstophosphoric heteropolyacid. *Russ. J. Inorg. Chem.* **2010**, *55*, 13–17. [[CrossRef](#)]
37. Oh, K.; Kwon, O.; Son, B.; Lee, D.H.; Shanmugam, S. Nafion-sulfonated silica composite membrane for proton exchange membrane fuel cells under operating low humidity condition. *J. Memb. Sci.* **2019**, *583*, 103–109. [[CrossRef](#)]
38. Kim, D.J.; Jo, M.J.; Nam, S.Y. A review of polymer-nanocomposite electrolyte membranes for fuel cell application. *J. Ind. Eng. Chem.* **2015**, *21*, 36–52. [[CrossRef](#)]
39. Gerasimova, E.; Safronova, E.; Ukshe, A.; Dobrovolsky, Y.; Yaroslavtsev, A. Electrocatalytic and transport properties of hybrid Nafion membranes doped with silica and cesium acid salt of phosphotungstic acid in hydrogen fuel cells. *Chem. Eng. J.* **2016**, *305*, 121–128. [[CrossRef](#)]
40. Xu, G.; Wei, Z.; Li, S.; Li, J.; Yang, Z.; Grigoriev, S.A. In-situ sulfonation of targeted silica-filled Nafion for high-temperature PEM fuel cell application. *Int. J. Hydrogen Energy* **2019**, *44*, 29711–29716. [[CrossRef](#)]
41. Yurova, P.A.; Tabachkova, N.Y.; Stenina, I.A.; Yaroslavtsev, A.B. Properties of ceria nanoparticles with surface modified by acidic groups. *J. Nanopart. Res.* **2020**, *22*, 318. [[CrossRef](#)]

42. Stenina, I.A.; Voropaeva, E.Y.; Brueva, T.R.; Sinel'nikov, A.A.; Drozdova, N.A.; Ievlev, V.M.; Yaroslavtsev, A.B. Heat-treatment induced evolution of the morphology and microstructure of zirconia prepared from chloride solutions during. *Russ. J. Inorg. Chem.* **2008**, *53*, 842–848. [[CrossRef](#)]
43. Agafonov, A.V.; Kraev, A.S.; Ivanova, O.S.; Evdokimova, O.L.; Gerasimova, T.V.; Baranchikov, A.E.; Kozik, V.V.; Ivanov, V.K. Comparative study of the electrorheological effect in suspensions of needle-like and isotropic cerium dioxide nanoparticles. *Rheol. Acta* **2018**, *57*, 307–315. [[CrossRef](#)]
44. Yurova, P.A.; Stenina, I.A.; Yaroslavtsev, A.B. A comparative study of the transport properties of homogeneous and heterogeneous cation-exchange membranes doped with zirconia modified with phosphoric acid groups. *Pet. Chem.* **2018**, *58*, 1144–1153. [[CrossRef](#)]
45. Calaza, F.C.; Chen, T.L.; Mullins, D.R.; Xu, Y.; Overbury, S.H. Reactivity and reaction intermediates for acetic acid adsorbed on CeO₂(1 1 1). *Catal. Today* **2015**, *253*, 65–76. [[CrossRef](#)]
46. Stenina, I.A.; Yurova, P.A.; Titova, T.S.; Polovkova, M.A.; Korchagin, O.V.; Bogdanovskaya, V.A.; Yaroslavtsev, A.B. The influence of poly(3,4-ethylenedioxythiophene) modification on the transport properties and fuel cell performance of Nafion-117 membranes. *J. Appl. Polym. Sci.* **2021**, *138*, 50644. [[CrossRef](#)]